Geomorphology 117 (2010) 78–89

Contents lists available at ScienceDirect

Geomorphology

journal homepage: www.elsevier.com/locate/geomorph

Thermochronological constraints on the long-term erosional history of the Karkonosze Mts., Central Europe

Martin Danišík [a,b,*], Piotr Migoń [c], Joachim Kuhlemann [a,d], Noreen J. Evans [b,e], István Dunkl [f], Wolfgang Frisch [a]

[a] Institute of Geosciences, University of Tübingen, Sigwartstraße 10, D-72076 Tübingen, Germany
[b] John de Laeter Centre of Mass Spectrometry, Applied Geology, Curtin University of Technology, GPO Box U1987, Perth WA 6845, Australia
[c] University of Wrocław, Department of Geography and Regional Development, pl. Uniwersytecki 1, 50-137 Wrocław, Poland
[d] ENSI, CH-5232 Villigen-ENSI, Switzerland
[e] CSIRO Exploration and Mining, ARRC, 26 Dick Perry Avenue, WA 6151, Australia
[f] Geoscience Center Göttingen, Sedimentology and Environmental Geology, Goldschmidtstrasse 3, D-37077 Göttingen, Germany

ARTICLE INFO

Article history:
Received 7 April 2009
Received in revised form 7 November 2009
Accepted 11 November 2009
Available online 18 November 2009

Keywords:
Apatite and zircon (U-Th-[Sm])/He dating
Apatite fission track dating
Karkonosze Mts.
Sudetes
Summit planation surface

ABSTRACT

A combination of zircon (U–Th)/He (ZHe), apatite fission track (AFT) and apatite (U–Th–[Sm])/He (AHe) thermochronology is used to constrain the long-term exhumation and erosional history of the Karkonosze Mts. in north-eastern Bohemian Massif by analyzing samples from the highly elevated summit planation surface. ZHe ages from the south-eastern part of the planation surface are 285 ± 19, 295 ± 20 and 308 ± 21 Ma, indicating that the area remained at temperatures below ~190 °C since the Permian. In contrast, ZHe ages in the western part of the planation surface are mid-Cretaceous, proving that this part was residing at temperatures above ~190 °C prior to exhumation. The exhumation occurred in the Late Cretaceous, as evidenced by AFT and AHe ages, ranging from 82 ± 5 to 90 ± 8 Ma and from 77 ± 5 to 91 ± 6 Ma, respectively.

Modelled cooling trajectories are characterized by a two-stage cooling history: fast cooling through the apatite partial annealing zone and helium partial retention zone to surface conditions between ~90 and ~75 Ma, and slow cooling or even thermal stagnation from ~75 Ma to present. Although our data do not allow us to resolve the age of the planation surface completely, we narrowed down the number of explanatory options and propose two alternative solutions for the formation of the planation surface: (i) the planation surface represents the remnant of a Permian peneplain, which was buried by Mesozoic sediments of the Central European Basin System and was re-exposed in the Late Cretaceous; or, (ii) the planation surface formed after ~75 Ma, after termination of a period of massive erosion documented by thermochronological data and by the sedimentary record in adjacent basins. Cenozoic relief production and uplift of the planation surface, evident from regional landforms and the sedimentary record, is not recorded by thermochronological data. This shows that erosion on the uplifted planation surface since ~75 Ma was less than ~1.2 km.

1. Introduction

Mountain ranges and uplands in Central Europe, particularly those within the Bohemian Massif, occupy a prominent position in the history of geomorphology. Some of the earliest advances in the understanding of continental geomorphology were born here: Penck (1925) developed the concept of *Rumpfflächen* and *Piedmonttreppen*, once considered the alternative to Davisian models of cyclic relief development; Jessen (1938) and Büdel (1957) built the fundamentals for historic climatic geomorphology, distinguishing different generations of landforms and landscapes.

Among the characteristic landforms in the Bohemian Massif are extensive tracts of planar relief at high elevation — the so-called 'summit planation surfaces'. They dominate the skylines of many individuals ranges and massifs at altitudes of up to 1200–1500 m a.s.l. and are usually considered to represent the oldest geomorphic elements in the present-day landscape. As prominent morphostratigraphic markers and excellent reference levels, the summit planation surfaces have a great potential for any attempts to decipher the long-term erosional history of mountain ranges. However, an essential problem with these surfaces, which undermines the credibility of any such attempts, is their unconstrained age. They are clearly erosional surfaces, truncating Variscan crystalline basement. This indicates that (i) a substantial, but largely unknown thickness of rock must have been eroded away since the late Palaeozoic and (ii) there is a vast window of time during which these elevated planar surfaces may have formed. Unfortunately, given

* Corresponding author. John de Laeter Centre of Mass Spectrometry, Applied Geology, Curtin University of Technology, GPO Box U1987, Perth WA 6845, Australia. Tel.: +61 8 9266 4680; fax: +61 8 9266 3153.
E-mail addresses: M.Danisik@curtin.edu.au (M. Danišík), pmigon@yahoo.com (P. Migoń), Joachim.Kuhlemann@ensi.ch (J. Kuhlemann), Noreen.Evans@csiro.au (N.J. Evans), istvan.dunkl@geo.uni-goettingen.de (I. Dunkl), frisch@uni-tuebingen.de (W. Frisch).

0169-555X/$ – see front matter © 2009 Elsevier B.V. All rights reserved.
doi:10.1016/j.geomorph.2009.11.010

the patchy knowledge of the sedimentary history of nearby basins, classic geomorphological methods are unable to constrain the erosional history of these basement massifs and put solid limits on the age of the summit planation surfaces (e.g., Désire-Marchand and Klein, 1987; Eitel, 2002).

Long used to reconstruct the thermal history of rocks at shallow crustal levels, low-temperature thermochronology can provide geomorphologists with a means to constrain long-term landform evolution (e.g., Brown et al., 1994; Summerfield, 2000). Apatite and zircon fission track data can provide temporal constraints in rapidly eroded orogens as well as in intraplate settings with lower erosion rates. Recently, fission track method has been complemented by the revived (U–Th–[Sm])/He dating method, further enhancing the potential of thermochronology in geomorphological studies (e.g., Belton et al., 2004; Foeken et al., 2007; Gunnell et al., 2009).

In this study we target the Karkonosze Mts. in north-eastern Bohemian Massif (Fig. 1) because of the following reasons: (i) there is a broad summit planation surface at 1300–1450 m a.s.l. (Fig. 2) forming a prominent component of the present-day topography; (ii) the Karkonosze Mts. is the highest mountain massif in the Bohemian Massif (highest peak: 1603 m a.s.l.), and second highest in the peri-Alpine belt of rejuvenated Variscan massifs, after the French Massif Central (Fig. 1); and (iii) to the south it is bordered by the Bohemian Cretaceous Basin, which records erosional and depositional history of the area.

Although a number of Bohemian Massif studies reported apatite fission track (AFT) ages (e.g., Wagner et al., 1989; Coyle et al., 1997; Hejl et al., 1997; Glasmacher et al., 2002; Ventura and Lisker, 2003; Aramowicz et al., 2006; Lange et al., 2008), thermochronology tools were seldom used to decipher geomorphic histories or validate conceptual models (such as that of Bischoff, 1993). In particular, combined AFT and (U–Th–[Sm])/He dating has not yet been applied in the Bohemian Massif in a geomorphic context.

Here we present original AFT, apatite (U–Th–[Sm])/He and zircon (U–Th)/He data (AHe and ZHe, respectively) measured on samples from the major summit planation surface in Karkonosze Mts. We seek to (i) reconstruct the low temperature thermal evolution of the Variscan basement that underlies this surface, (ii) constrain its long-term exhumation and erosion history; and (iii) derive constraints on the age of the summit planation surface. We do so by modelling thermal trajectories from measured data, trying to identify and bracket episodes of fast and slow cooling, that may correspond to the phases of exhumation and planation, respectively.

2. Study area

The Karkonosze Mts. are located in the West Sudetes, which themselves are a mountain range, bordering the Bohemian Massif on its north-eastern side (Fig. 1). They rise above the piedmont plain to the north by more than 1000 m, and the elevation difference with respect to the central part of the Bohemian Massif is of the same order. Topographically, the Sudetes represent a mosaic of horst-like blocks and depressions, often separated by distinct escarpments, resulting from differential uplift and subsidence in the late Cenozoic (e.g., Klimaszewski, 1958; Demek, 1975; Dyjor and Dyjor, 1975).

2.1. Geological setting

The main mountain-building phase for the Sudetes occurred during the Variscan orogeny in the Late Devonian/Early Carboniferous (Aleksandrowski and Mazur, 2002; Mazur et al., 2006). The main orogenic phase was accompanied by enhanced magmatic activity that produced the Karkonosze-Jizera Pluton (Rb–Sr whole rock isochron ages from 310 ± 14 to 329 ± 17 Ma; Duthou et al., 1991), the major component of the Karkonosze Mts. (Fig. 3; Mazur et al., 2007). The

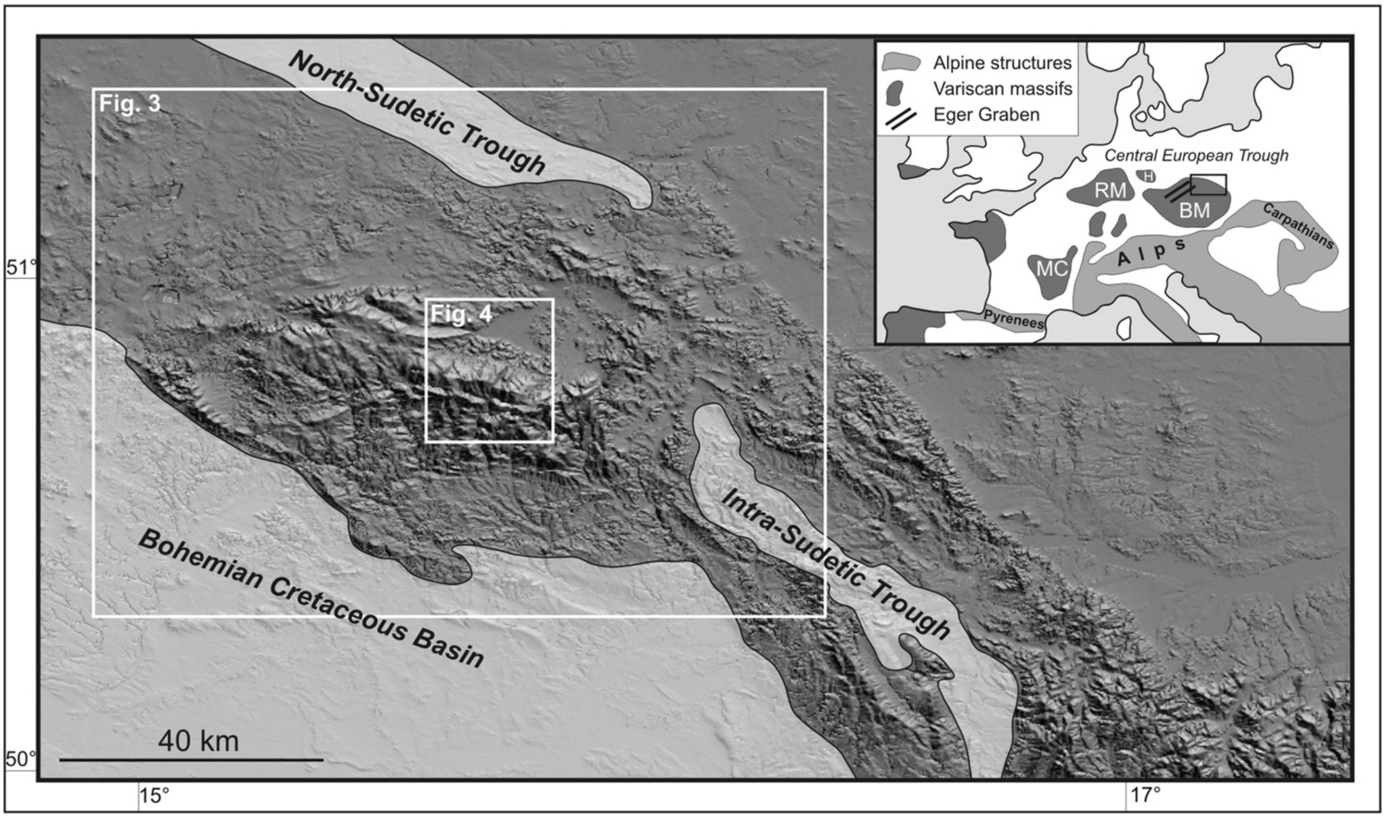

Fig. 1. Location of the study area within the Sudetes and in relation to Alpine and Variscan structures in central and western Europe. Areas indicated in white show the current extent of Upper Cretaceous sediments. Abbreviations in the inset: BM - Bohemian Massif, H - Harz Mts., MC - Massif Central, RM - Rhenish Massif.

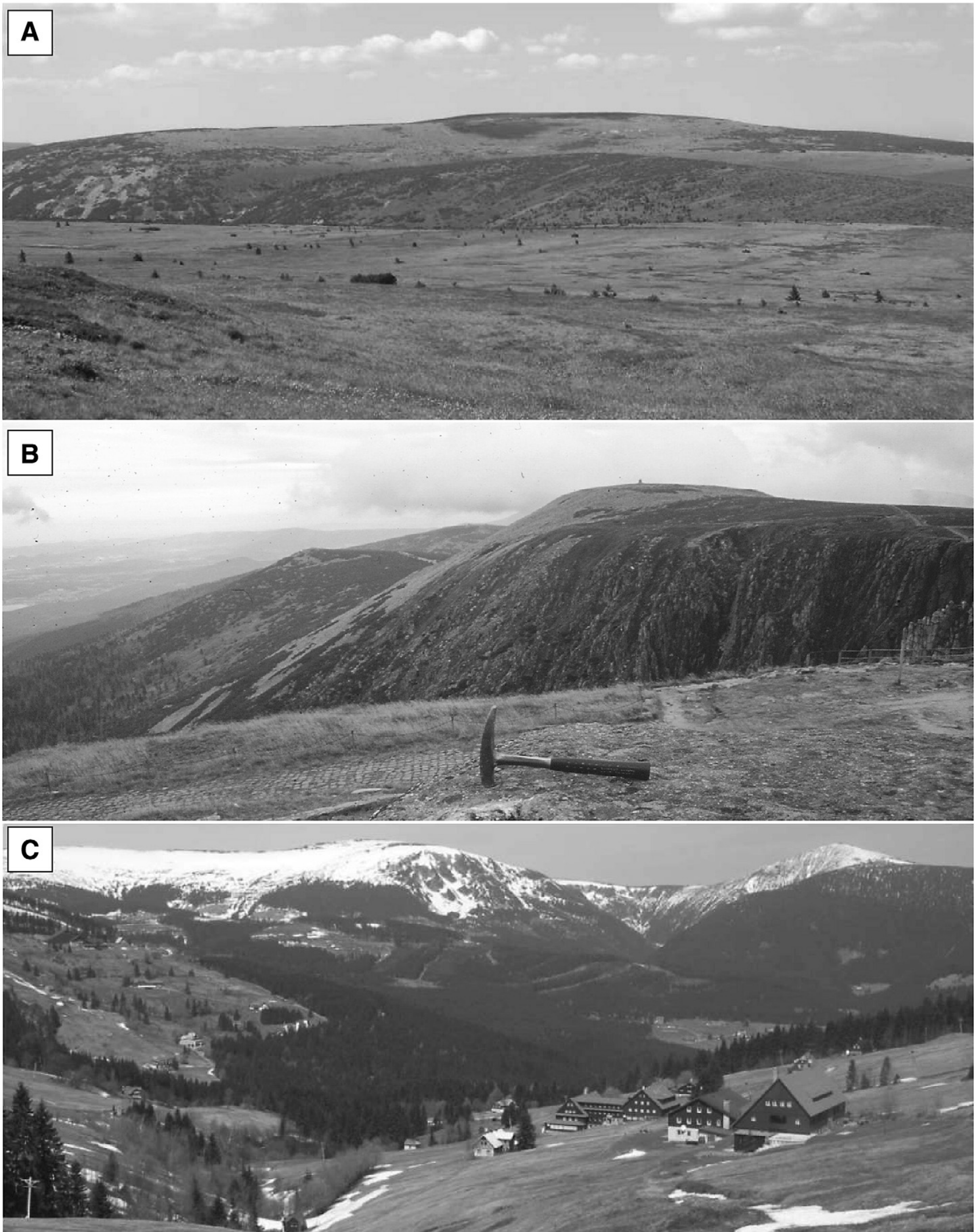

Fig. 2. Main topographic elements of the Karkonosze Mts. A, B — summit planation surface at ~1500 m a.s.l.; C — heavily dissected southern slopes, summit planation surface forms the skyline.

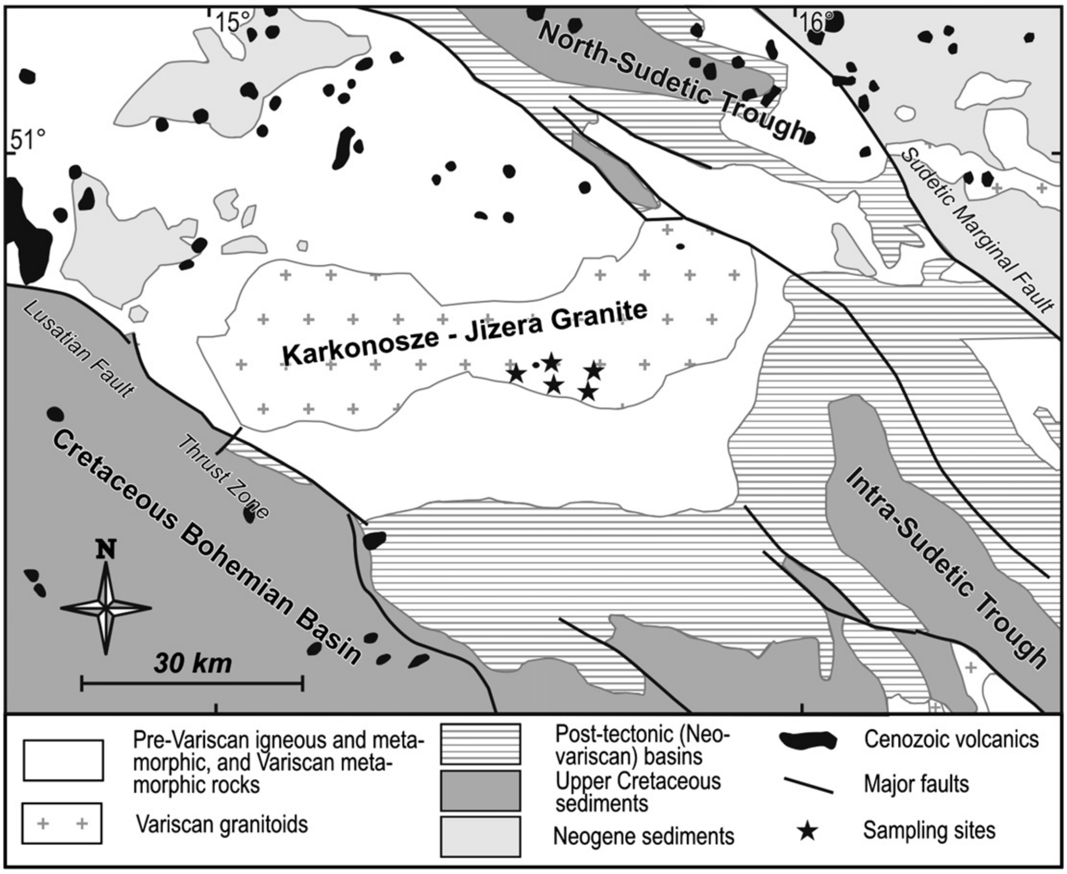

Fig. 3. Simplified geological map of the Karkonosze Mts. and adjacent area (modified after Maheľ, 1973; Kozdrój et al., 2001).

depth of emplacement is estimated to be 7–8 km from thermobarometric data (Dudek and Suk, 1965).

Successive unroofing and erosion of the Karkonosze granite took place in the Early Permian (Saxonian), as evidenced by large volumes of coarse clastic deposits preserved south, east, and north of the Karkonosze (Fig. 3; Berg, 1938). It is likely that by the end of Permian the area was largely planed off, as inferred from the nature of Upper Permian sediments preserved in the above-mentioned areas of deposition. These are siltstones, fine-grained sandstones, caliche and gypsum horizons (Śliwiński, 1980), as well as limestones, dolomites and marls of marine origin. Sandy sedimentation typified the Early Triassic and carbonate sedimentation the Middle Triassic (Chrząstek, 2002). No sedimentary record for Late Triassic–Early Cretaceous period exists either inside or around the Sudetes. Migoń and Lidmar–Bergström (2001) presumed that during this period the Bohemian Massif, including the West Sudetes, underwent slow-going surface lowering, with a significant role of deep weathering and formation of thick weathering mantles over Palaeozoic basement rocks. However, since no weathering residuals from this period are reported from the Karkonosze Mts., the geological history of the massif between ~230 Ma and ~90 Ma remains unclear.

Sedimentation resumed in the early Late Cretaceous (Cenomanian), when a Bohemian Cretaceous Basin System formed (Skoček and Valečka, 1983). The basin system comprised several pull-apart sub-basins filled with marine sediments, ranging from nearshore fine gravels through thick, massive cross-bedded sandstones to mudstones and marls. A major part of the sediments deposited around the Karkonosze area is represented by Turonian sandstones (Skoček and Valečka, 1983; Wojewoda, 1997; Uličný, 2001). The youngest sediments in the Intra-Sudetic Trough, North-Sudetic Trough and Bohemian Cretaceous Basin (Fig. 3) are of Turonian (~90 Ma), Santonian (~80 Ma) and Coniacian age (~86 Ma), respectively. It is not clear whether the entire West Sudetes were ever buried beneath Cretaceous sediments.

At the Cretaceous/Paleogene boundary, the entire region was affected by regional transpression leading to inversion of Cretaceous basins, local upthrusting of basement blocks in the Bohemian Massif and the inverse reactivation of numerous former extensional faults (Coubal, 1990; Uličný et al., 2003; Mazur et al., 2005; Ziegler and Dèzes, 2007). The Lusatian Fault Thrust Zone, which separates the basement block of the West Sudetes from the Cretaceous Bohemian Basin, was clearly active during this period, accounting for brittle deformation of Cretaceous (Cenomanian) rocks (Coubal, 1990; Uličný et al., 2003).

In the Middle Eocene, a NE-striking Eger rift evolved as a part of the European Cenozoic Rift System (Dèzes et al., 2004), and related volcanic activity lasted from Late Eocene to Early Miocene times (~35–20 Ma) in the area (e.g., Adamovič and Coubal, 1999; Ulrych et al., 1999; Badura et al., 2005). Sedimentation in tectonic grabens north and south of the Sudetes commenced in the Early Miocene (Prosová, 1974; Dyjor and Dyjor, 1975), but no comparable deposits were found within the Sudetes. There is a coarse gravel deposition starting in the latest Miocene (~7–5 Ma), which is preceded by the widespread deposition of clay and silt around the Sudetes (Dyjor, 1970; Badura and Przybylski, 2004). In the middle Pleistocene, the topography of the Karkonosze Mts. was evidently similar to that of the present, dictating the pattern of local mountain glaciation (Partsch, 1894; Migoń, 1999).

2.2. Geomorphic features

Geomorphological analysis of the Karkonosze Mts. reveals several major landscape elements, such as the extensive summit surface of low relief, adjacent hills made up of more resistant granite, straight escarpments outlining the boundaries of the massif, deeply incised valleys, particularly near the southern margin, and long north-facing slopes of the main watershed ridge (Figs. 2, 4). However, the ages of these elements are virtually unknown and broad age assignments

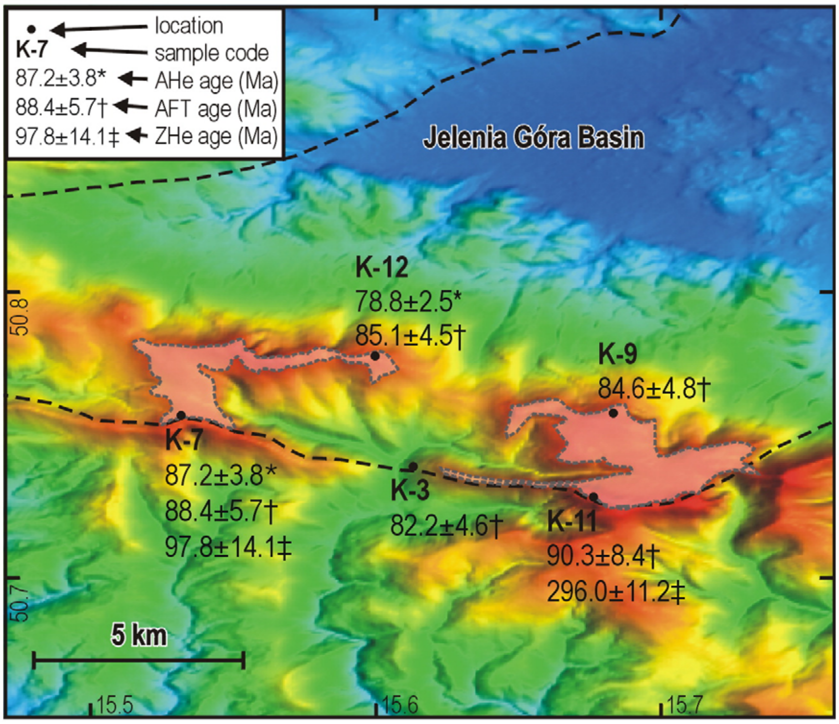

Fig. 4. DEM of the Karkonosze Mts. with position of the summit planation surface (grey dashed lines) and measured AHe, AFT and ZHe ages. Area between thick black dashed lines consists of granite.

present in the literature are largely speculative. Currently the most common view, traced back to Sekyra (1964), is that the summit plain is a remnant of an early Cenozoic (Palaeogene) peneplain which was dissected along faults, differentially uplifted and/or tilted in the Neogene, and incised by rivers since then. But no thermochronological or other evidence has ever been presented to justify these speculations.

3. Previous studies on long-term denudation of the Karkonosze Mts.

Skoček and Valečka (1983) attempted to estimate the sediment volume contained in Upper Cretaceous sandstones in the northern part of the Bohemian Cretaceous Basin. These authors concluded that ~2000 km^3 of sediment is preserved and argued that 700 m of denudation of the 'West Sudetic Island' (which includes the area of Karkonosze) was required to account for this volume. This value, however, should be considered as a minimum estimate for at least two reasons. First, an unknown proportion of sediment was exported to distal sinks, including a large part of the silt fraction, most of the clay and virtually all of the dissolved load. If the Alps were used as an analogue, this portion would make up at least half of the total budget (Kuhlemann, 2000). Second, an unknown thickness of Cretaceous sediment was lost during post-depositional erosion.

Another attempt to reconstruct the exhumation and erosion history of the Karkonosze granite and to derive long-term denudation rates was presented by Mierzejewski (1985). The interpretations were based on the assumption that ~3.5 km of granite has been removed since unroofing and that ~2.2 km had been eroded since the Turonian. The former figure arises from a tentative reconstruction of the original shape of the pluton based on magmatic foliation and geological cross-sections provided by Cloos (1925), whereas the latter results from an interpretation of a single 94 Ma AFT age from the marginal part of the pluton (Jarmołowicz-Szulc, 1984), assuming that the mean geothermal gradient in the last 100 Myr was 40 °C/km. Mierzejewski (1985) suggested a possible increase in denudation rates towards the later Cenozoic, as a side-effect of faulting and uplift in the Neogene, but did not consider any phases of accelerated denudation earlier in the Cenozoic or in the Mesozoic. Overall, the multiple assumptions inherent in the approach, the paucity of thermochronological data and the reliance on primarily circumstantial evidence do not provide a solid basis for the proposed scenario.

4. Samples and methods

Four samples of granite were taken from the major summit planation surface for thermochronological investigation (Tables 1, 2; Fig. 4). One additional sample (K-3) was taken from a slope ~500 m below the planation surface.

Apatites and zircons were separated using conventional magnetic and heavy liquid techniques. Fission track analysis was carried out in the Thermochronological Laboratory of the University of Tübingen (Germany) using standard procedures described in Danišík et al. (2007). The external detector method (Gleadow, 1981) was applied with the etching protocols of Donelick et al. (1999) for apatite (5.5 M HNO_3 for 20 s at 21 °C). The zeta calibration approach (Hurford and Green, 1983) was adopted to determine the age. AFT ages were calculated using TrackKey 4.2g (Dunkl, 2002). Where possible, up to 100 horizontal confined tracks were measured in prismatic grains of each sample, while distinguishing between TINTs (track in track) and TINCLEs (track in cleavage). The annealing properties of apatite were assessed by measurement of Dpar values (Dpar — the mean etch pit diameter of fission tracks on prismatic surfaces of apatite; e.g., Burtner et al., 1994).

For (U–Th–[Sm])/He analysis, apatite and zircon crystals were hand-picked following strict selection criteria (Farley, 2002; Reiners, 2005), then photographed and measured. Apatite was loaded in Pt tubes, degassed at ~960 °C under vacuum using laser-heating and analysed for ^4He using a Pfeiffer Prisma QMS-200 mass spectrometer in the Thermochronological Laboratory of the University of Tübingen. Following He measurements, the apatite was spiked with ^{233}U and ^{230}Th dissolved in nitric acid and analysed by isotope dilution inductively coupled mass spectrometry (ID ICP MS) for U, Th and

Table 1
Apatite fission track results.[a]

Sample code	Lat. (WGS-84)	Lon. (WGS-84)	Elev. (m a.s.l.)	Lithology	N	ρ_s	N_s	ρ_i	N_i	ρ_d	N_d	$P(\chi^2)$ (%)	Age (Ma)	± 1σ (Ma)	MTL (µm)	SD (µm)	N (L)	Dpar (µm)
K-3	50.7420	15.6103	831	granite	20	9.961	761	10.340	790	5.324	3675	>95	82.2	4.6	13.2	1.3	100	1.7
K-7	50.7568	15.5354	1382	granite	24	6.162	559	6.074	551	5.436	3675	>95	88.4	5.7				1.8
K-9	50.7596	15.6828	1400	granite	25	7.702	732	7.660	728	5.249	3675	>95	84.6	4.8	13.4	1.3	73	1.7
K-11	50.7286	15.6795	1537	granite	20	3.548	253	3.422	244	5.436	3675	>95	90.3	8.4				1.6
K-12	50.7771	15.6015	1378	granite	25	7.101	855	8.072	972	6.036	3675	>95	85.1	4.5				1.7

[a] N — number of dated apatite crystals; ρ_s (ρ_i) — spontaneous (induced) track densities (×10^5 tracks/cm^2); N_s (N_i) — number of counted spontaneous (induced) tracks; ρ_d — dosimeter track density (×10^5 tracks/cm^2); N_d — number of tracks counted on dosimeter; $P(\chi^2)$ — probability obtaining Chi-square value (χ^2) for n degree of freedom (where n = No. of crystals − 1); Age ± 1σ — central age ± 1 standard error (Galbraith and Laslett, 1993); MTL — mean track length; SD — standard deviation of track length distribution; N (L) — number of horizontal confined tracks measured; Dpar — average etch pit diameter of fission tracks. Ages were calculated using zeta calibration method (Hurford and Green, 1983), glass dosimeters CN-5, and zeta values of 322.71 ± 5.3 year/cm^2.

Sm at the Geoscience Center Göttingen (Germany) on a Perkin Elmer (ELAN DRC II) ICP-MS. Zircon was loaded in Nb tubes, degassed at ~1250 °C and analysed for ^{4}He using the CSIRO Exploration and Mining extraction line in the John de Laeter Centre of Mass Spectrometry in Perth (Australia). Degassed zircon was dissolved following the procedure of Evans et al. (2005) and analysed by ID ICP MS for U and Th at TSW Analytical Ltd in the University of Western Australia (Perth) on an Agilent 7500 mass spectrometer. For more details on analytical procedures, the reader is referred to Evans et al. (2005) and Danišík et al. (2008).

Total analytical uncertainty (TAU) was computed as the square root of the sum of the squares of weighted uncertainties on U, Th, Sm and He measurements. TAU was less than ~5 % in all cases and was used to calculate the error of raw (U–Th–[Sm])/He ages. The raw AHe and ZHe ages were corrected for alpha ejection (Ft correction) after Farley et al. (1996) and Hourigan et al. (2005), respectively. A value of 5% was adopted as the uncertainty on the Ft correction, and was used to calculate errors for the corrected AHe and ZHe ages (Table 2).

The low-temperature thermal history based on AFT and (U–Th–[Sm])/He data was modelled using the HeFTy modelling program (Ketcham, 2005) operated with the multikinetic annealing model of Ketcham et al. (1999) and the diffusion kinetics of the Durango apatite after Farley (2000) and zircon after Reiners et al. (2004).

5. Results and interpretation

The results of the AFT and (U–Th–[Sm])/He analyses are summarized in Tables 1 and 2 and shown in Fig. 4. AFT ages are reported as central ages with 1σ errors.

5.1. Zircon (U–Th)/He data

Zircon from two samples was dated by (U–Th)/He. Sample K-11 from the south-eastern part of the planation surface yielded three reproducible ZHe ages (285 ± 19; 295 ± 20; 308 ± 21 Ma), corresponding to the Carboniferous-Permian boundary. The ZHe ages are slightly younger than Rb–Sr ages of the pluton (310 ± 14 to 329 ± 17 Ma; Duthou et al., 1991), thus we interpret them as cooling ages, recording the passage of the granite through the zircon helium partial retention zone (ZHe PRZ: ~200–160 °C; Reiners et al., 2004). The cooling was probably related to post-orogenic unroofing of the pluton, which reached surface and was eroded in the Early Permian (Saxonian) as evidenced by granitic pebbles in the Intrasudetic Trough (Berg, 1938). Assuming a geothermal gradient of 30 °C/km, surface temperature of 10 °C and closure temperature of ~190 °C for ZHe system, the ZHe indicates that a maximum erosion of <6 km occurred during post-Permian times.

Table 2
(U–Th–[Sm])/He results.[a]

Sample code	N_c	Th (ng)	Th error (%)	U (ng)	U error (%)	Sm (ng)	Sm error (%)	He (ncc at STP)	He error (%)	TAU (%)	Th/U	Unc. age (Ma)	± 1σ (Ma)	Ft	Cor. age (Ma)	± 1σ (Ma)
Zircon																
K-7#1	1	12.738	5.3	41.423	4.5	n/a	n/a	400.705	1.8	4.9	0.31	73.7	3.6	0.86	85.9	6.0
K-7#2	1	13.588	5.3	42.251	4.4	n/a	n/a	565.977	2.0	4.9	0.32	101.5	5.0	0.86	117.8	8.3
K-7#3	1	17.428	5.3	44.118	4.3	n/a	n/a	452.642	1.8	4.8	0.39	76.7	3.7	0.85	90.6	6.3
K-7#4	1	14.726	5.3	47.914	4.7	n/a	n/a	520.625	0.6	4.8	0.31	82.7	4.0	0.85	96.8	6.7
Average (Ma) ± Std. dev. (Ma)															97.8 ± 14.1	
K-11#2	1	0.545	5.3	1.853	4.3	n/a	n/a	54.534	0.7	4.4	0.29	221.9	9.8	0.75	295.1	19.7
K-11#3	1	0.502	5.3	1.287	4.3	n/a	n/a	41.496	0.7	4.4	0.39	237.8	10.5	0.77	307.7	20.5
K-11#4	1	0.851	5.3	1.671	4.3	n/a	n/a	46.387	0.6	4.5	0.51	200.4	8.9	0.70	285.3	19.1
Average (Ma) ± Std. dev. (Ma)															296.0 ± 11.2	
Apatite																
K-7#1	1	0.155	2.4	0.097	2.1	0.9	11.2	0.815	0.9	3.4	1.60	50.4	1.7	0.60	83.5	5.1
K-7#2	1	0.088	2.4	0.051	2.6	1.2	11.8	0.599	0.9	4.7	1.71	68.4	3.2	0.75	91.2	6.3
K-7#4	1	0.180	2.4	0.118	2.0	1.1	12.3	1.241	0.9	3.6	1.52	63.5	2.3	0.73	87.0	5.4
Average (Ma) ± Std. dev. (Ma)															87.2 ± 3.8	
K-12#1	1	0.114	2.4	0.073	2.2	0.7	12.8	0.615	0.9	3.8	1.57	50.6	1.9	0.62	81.6	5.1
K-12#4	1	0.107	2.4	0.061	2.4	0.8	14.2	0.536	0.9	4.5	1.75	51.2	2.3	0.66	78.1	5.3
K-12#5	1	0.128	2.4	0.076	2.2	0.8	14.6	0.640	0.9	4.2	1.68	49.6	2.1	0.65	76.8	5.0
Average (Ma) ± Std. dev. (Ma)															78.8 ± 2.5	

[a] N_c — number of dated apatite crystals; Th — ^{232}Th; U — ^{235}U + ^{238}U; Sm — ^{147}Sm; He — ^{4}He; TAU — total analytical uncertainty; Unc. age — uncorrected He age; Ft — alpha recoil correction factor after Farley et al. (1996) an Hourigan et al. (2005); Cor. age — corrected He age.

In contrast, sample K-7 from the western part of the planation surface yielded three mid-Cretaceous ZHe ages (86 ± 6; 91 ± 6; 97 ± 7 Ma) showing that this part of the area was residing at temperatures above ~190 °C during Mesozoic times. This implies that the thickness of overburden must have exceeded ~6 km (assuming the same parameters as above), which is almost twice that suggested by Mierzejewski (1985) for the Late Permian, entire Mesozoic and Cenozoic combined (see Section 3).

5.2. Apatite fission track and apatite (U–Th–[Sm])/He data

The samples revealed one distinct age cluster of Late Cretaceous age: AFT and AHe ages range from 82 ± 5 to 90 ± 8 Ma and from 77 ± 5 to 91 ± 6 Ma, respectively. All samples yielded narrow AFT age spectra passing the chi-square test (Table 1) and are therefore considered to form one age population. The average Dpar value for all samples is ~1.7 µm (Table 1), indicating fluorine-rich apatite, typified by relatively low annealing temperature (~60–120 °C; e.g., Wagner and Van den haute, 1992; Ketcham et al., 1999). Track length distributions are unimodal, narrow (SD: 1.3 and 1.3 µm), negatively skewed, with relatively short mean track lengths (MTL: 13.2 and 13.4 µm) and relatively large standard deviations (Fig. 5).

Two samples contained apatite crystals suitable for (U–Th–[Sm])/He analysis (Table 2). AHe ages reproduce well and are slightly younger than, or indistinguishable from, the corresponding AFT, indicating rapid cooling through the apatite partial annealing zone and apatite helium partial retention zone (APAZ and AHePRZ, respectively; e.g., Wagner and Van den haute, 1992; Wolf et al., 1998).

To better reveal the meaning of the data, thermal histories were modelled based on available thermochronological data. In the best case, the thermal model for each sample should be constrained by ZHe, AHe and AFT age and length data. Unfortunately, the quality of the samples did not allow us to do so, as the samples where the number of confined tracks could be measured did not contain any apatite crystal of sufficient quality required for (U–Th–[Sm])/He dating. In addition, vice versa, it was not possible to measure track lengths in samples with apatite crystals suitable for (U–Th–[Sm])/He dating. Nevertheless, cooling trajectories were modelled for all samples, revealing fairly similar patterns (Fig. 6).

Modelled cooling trajectories are characterized by a two-stage cooling history: fast cooling through the APAZ and AHePRZ to surface conditions between ~90 and ~75 Ma followed by slow cooling or thermal stagnation lasting from ~75 Ma until present (Fig. 6). Unfortunately, the limited resolution of the modelled trajectories does not permit precise temporal constraints to be placed on the onset of the second phase. Considering the youngest AHe ages obtained, the variation point can be placed into the time interval ~85–75 Ma.

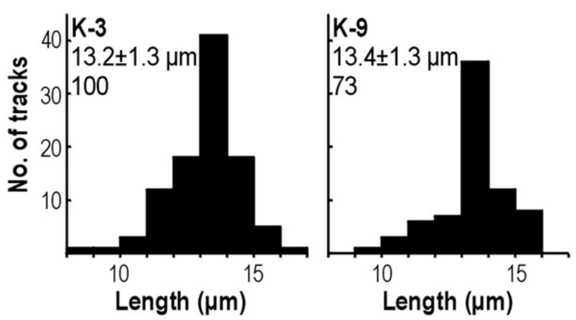

Fig. 5. Confined track length distributions of measured samples. Text from the top: sample code; mean track length ± standard deviation (both in µm); number of measured tracks.

6. Discussion

6.1. Long-term erosion history of the Karkonosze

The long-term exhumation and erosional history of the Karkonosze granite can be constrained by translation of the modelled cooling trajectories into exhumation rates, assuming a reasonable palaeo-geothermal gradient. Present-day geothermal gradient in the Karkonosze Mts. is about 30 °C/km, as estimated from surface heat flow (~60 mWm^{-2}; Bruszewska, 2000) and thermal conductivity data (2 Wm^{-1} K^{-1}; Žák et al., 2006). Adopting this value results in average exhumation rates of ~300 m/Ma between 90–75 Ma, and ~7 m/Ma between ~75 Ma and the present. Considering the limited resolution of the modelled cooling path, maximum and minimum exhumation rates for the fast cooling stage can range from ~1000 to ~100 m/Ma, and from ~16 to <0.1 m/Ma for the slow cooling stage. An important point to note is that regardless of the exact values of exhumation rates, the two stages differ by one to three orders of magnitude (see middle panel in Fig. 7). This further implies that since mid-Cretaceous at least 3.6 km and, as evidenced by ZHe data, at some places >6 km of overburden has been removed, with the majority (≥2.6–5 km) being eroded between 100–75 Ma and less than 1.2 km afterwards.

Fast cooling early in the Late Cretaceous indicates creation of topographic relief and rapid erosion. This interpretation is consistent with massive deposition of clastic sediments in the nearby Bohemian Cretaceous Basin during the latest Cenomanian to the Coniacian, now represented by thick sandstone sequences stretching along the south-western margin of the Sudetes (Figs. 1, 3). The period of vigorous erosion lasted at least for ~15 Ma and may have completely erased any elements of post-Variscan morphology in the Karkonosze.

The onset of the subsequent thermal stagnation period was constrained to ~85–75 Ma by thermal modelling results and the youngest AHe ages. This is in good agreement with the sedimentary record, which terminates at the beginning of the Santonian (~85 Ma ago) in the Bohemian Cretaceous Basin, but in the North Sudetic Trough north of the Karkonosze sedimentation continued well into the Santonian and upward-fining of material is evident (Milewicz, 1997).

The post-75 Ma period of thermal stagnation can be interpreted as a time span during which the denudation system reached a low-energy state and the previous topography decayed into a low relief surface, transformed by erosion at a very low rate. Again, this interpretation is supported by the sedimentary record around the Sudetes. No Palaeocene or Eocene sediments are found, implying very low sediment fluxes, perhaps with the predominance of solute export. Hilly areas and rolling plains in the present-day tropics and sub-tropics are characterised by very low denudation rates (e.g., von Blanckenburg et al., 2004) and are probable analogues to the Karkonosze Mts. and the Sudetes in the early Cenozoic.

The geomorphic history of the Neogene is puzzling and thermo-chronological data are difficult to interpret unequivocally. The present-day Karkonosze shows considerable relief and altitude, indicating that a major change occurred after the early Cenozoic gentle relief had been created. This is usually attributed to differential uplift, which occurred along the northern rim of the Bohemian Massif in response to crustal stresses transmitted from the Alps, Carpathians and/or Pyrenees (Malkovský, 1987; Faupl and Wagreich, 1999; Badura et al., 2007; Zuchiewicz et al., 2007). This is consistent with enhanced deposition in grabens and foreland areas located north of the Sudetes (Dyjor and Dyjor, 1975), indicating resumed erosion and transport at a larger scale. Deposition in the foreland continued throughout the Pliocene into the Quaternary, corresponding to an increase in mean grain size in the sediment. The origin of this coarsening has been variously attributed to an increase in hillslope gradients due to uplift of the source area or an increase in the availability of coarse material due to climate deterioration, or both (Badura and Przybylski, 2004).

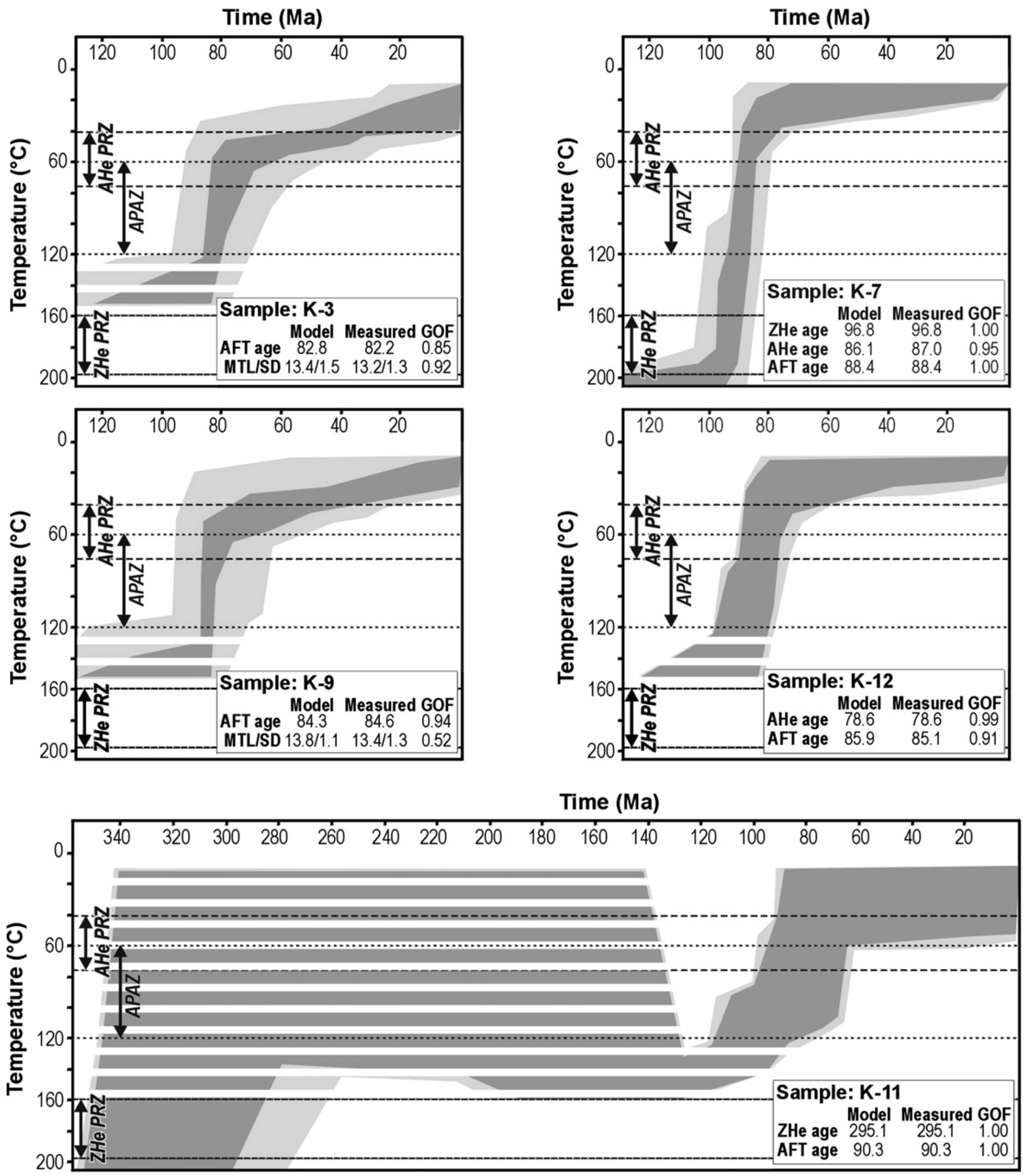

Fig. 6. Thermal modelling results of available thermochronological data displayed in time–temperature diagrams. The HeFTy modelling program (Ketcham, 2005) was operated with the multikinetic annealing model of Ketcham et al. (1999) and the diffusion kinetics of the Durango apatite after Farley (2000) and zircon after Reiners et al. (2004). Light grey envelopes indicate 'acceptable fit'; dark grey envelopes indicate 'good fit'; horizontal hatching indicate areas with uncertain thermal history; AHe PRZ — apatite helium partial retention zone; APAZ — apatite partial annealing zone; ZHe PRZ — zircon helium partial retention zone; MTL/SD — mean track length and standard deviation in μm; GOF is goodness of fit (statistical comparison of the measured input data and modelled output data, where a "good" result corresponds to value 0.5 or higher, the best result corresponds to value 1). Depending on the availability of input parameters, the samples were modelled as follows: samples K-3 and K-9 were modelled using AFT age and track length data. The rest of the samples (K-7, K-11, K-12) was modelled using AHe and/or ZHe data and AFT age data without track lengths, where AFT age was assumed to be a cooling age as inferred from track length distributions and cooling paths revealed by samples K-3 and K-9.

However, our modelled cooling paths do not indicate any accelerated cooling that would be consistent with the production of new topographic relief, as is inferred from geomorphological analysis and evidenced in the Neogene sedimentary record. There are two possible ways to explain this. First, the contemporary topographic relief may be very young (Plio-Pleistocene?), so the effect of erosion achieved so far would be too small to impart a change on the thermochronological record. Alternatively, the production of relief may have started earlier (e.g., in the Early to Middle Miocene as suggested by Ziegler and Dèzes (2007)), but the subsequent erosion was very slow so that cumulative exhumation was limited. An important factor in the discussion is the adjacent intramontane basin of Jelenia Góra (Fig. 4), which, despite being an almost closed basin, is lacking sediments that can be correlated with significant erosion in the Karkonosze. Apart from a thin (2–4 m) veneer of gravel and sand along main rivers, the floor of the basin cuts across granite bedrock. Glacial deposits in the northern part of the basin are a result of Scandinavian ice sheet advance and are unrelated to the long-term denudation of the Karkonosze.

Straight marginal escarpments of tectonic origin (not yet transformed into highly sinuous residual fault scarps; see Bull and McFadden, 1977), irregular stream profiles, and the absence of thick correlative

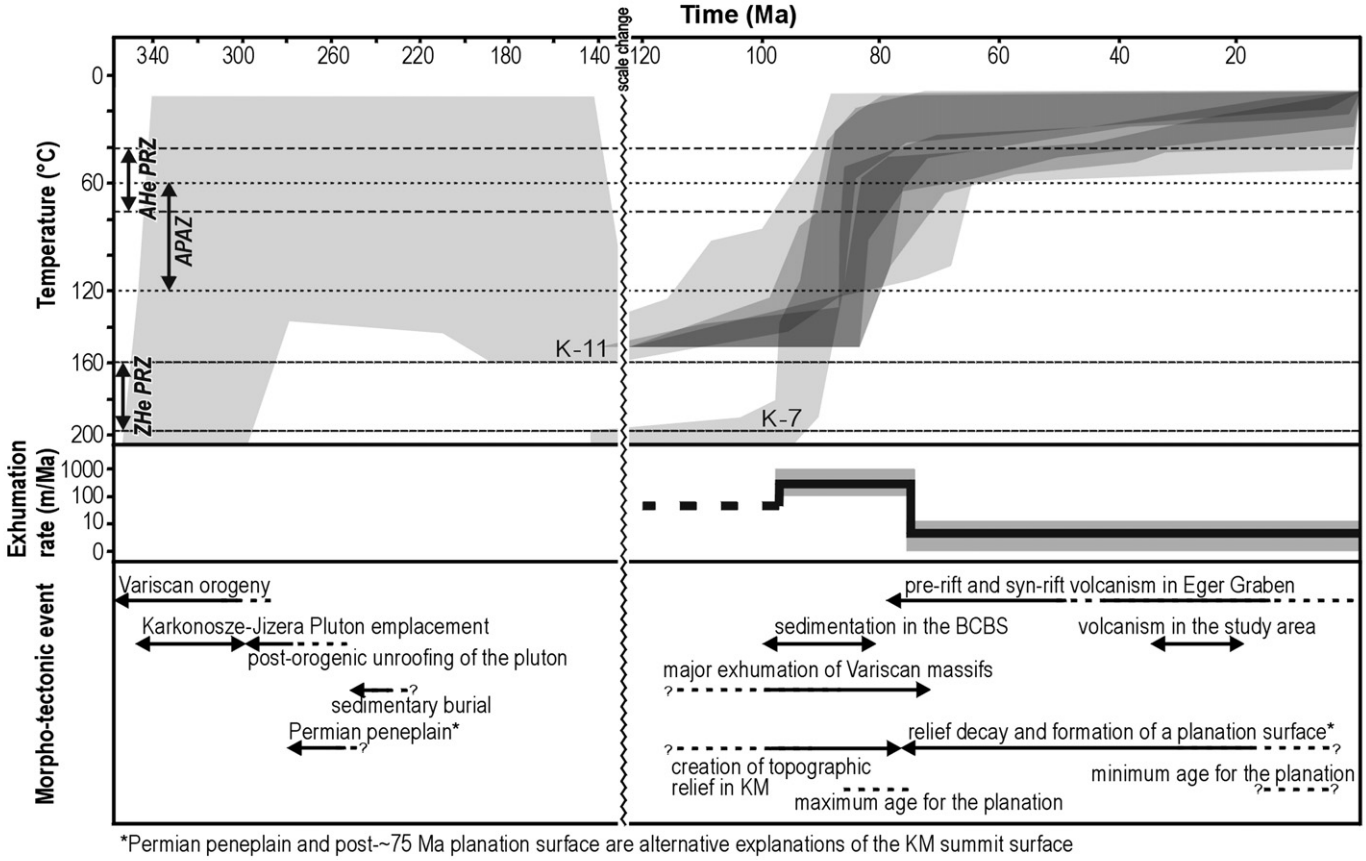

Fig. 7. Upper diagram: time–temperature diagram showing superimposed 'good fit' thermal trajectories of all samples adopted from Fig. 6. Middle diagram: corresponding average exhumation rates (black lines) with associated errors (grey envelopes). Lower diagram: major morpho-tectonic events in the study area, surrounding regions and adjacent Variscan massifs. BCBS — Bohemian Cretaceous Basin System; KM — Karkonosze Mts. Note that summit planation surface can explained as a remnant of either a Permian peneplain or post-~75 Ma planation surface. See text for further explanation.

deposits both north and south of the Karkonosze appear more consistent with the first hypothesis. If this is accepted, and the topographic relief of the Karkonosze is attributed solely to Pliocene–Pleistocene events, the corresponding rate of surface uplift would need to be at least 200 m in one million years. However, there are also convincing arguments to suggest that the intensity of erosion may have indeed been moderate even in the long term. Granite is one of the mechanically strongest rocks present in the Sudetes (Placek and Migoń, 2007), and is therefore fairly resistant to physical weathering and erosion. Moderate uplift, typical for intraplate settings and inferred for the Sudetes, does not necessarily create very steep slopes and bedrock landslides (one of the major agents of rapid denudation in areas subject to high rate of uplift) do not occur. Terrain observations, historical records and limited quantitative data all indicate that the present Karkonosze Mts. have been transformed by surface processes at a slow rate, with localized debris flows being the only major geomorphic events (Migoń et al., 2002). These circumstances leave the scope for more protracted uplift and low long-term rates of erosion, not necessarily contradicting the regional model by Ziegler and Dèzes (2007) (see below).

6.2. Constraints on the age of planation surfaces

As discussed in Section 2, the age of the summit planation surfaces of the Karkonosze Mts. is still a matter of debate. The thermochronological data cannot resolve the problem completely, but are able to constrain the age of the summit planation surface in a way that has not been attempted before (see also Fig. 7).

An age for planation can be determined from thermal trajectories by bracketing the episodes slow cooling or thermal stagnation, which corresponds to the phases of planation. In clear-cut cases, the thermal stagnation episodes are delimitated by fast cooling episodes, corresponding to tectonic events. This is not the case here and interpretation depends on the preferred genetic hypothesis.

For instance, it could be argued that the Permian ZHe ages in the eastern part of the Karkonosze Mts. reflect formation of a Permian peneplain, common in the Variscan massifs of Europe, which has since been buried by Upper Permian, Triassic and perhaps even Jurassic sediments at the southern margin of the Central European Basin System. Burial by less than 5 km thickness in the eastern part and by more than 5 km in the western part, assuming a thermal gradient of 30 °C/km, may reflect some regional tilting, but a degree of heterogeneity of heat flow during maximum burial could also explain the observation. Regional basin inversion and uplift in the Polish part of the Central European Basin System between ~85 and ~65 Ma is well established (Krzywiec, 2006; Resak et al., 2008), and fast erosion of a hypothetical sedimentary cover related to the Variscan unconformity in the study area is more plausible than fast erosion of granite, as found in the western Mediterranean (Danišík, 2005). This implies that a peneplain formed in the Permian and was buried by Mesozoic sediments until the mid-Cretaceous with uplift triggering fast erosion and exposing the Variscan unconformity by ~85–75 Ma.

Alternatively (and perhaps more likely), the formation history of the planar relief is entirely post-mid-Cretaceous and is connected with the decay of substantial topographic relief, which existed in the Turonian and Coniacian and supplied detritus into the adjacent sedimentary basins. Our thermochronological record of fast erosion ends at ~75 Ma, which can understood as maximum age of the planation surface. The minimum age constraint for the planation surface is equivocal. The present-day tectonic topography evidently post-dates the planar relief, but neither thermochronological cooling paths nor sedimentary record allow us to bracket its age with certainty. If the regional scenario by Ziegler and Dèzes (2007) is adopted, then the period after 18 Ma ago was no longer conducive to planation. If the topographic relief of the Karkonosze Mts. is considered as young as Plio-Pleistocene, then planation of relief may have continued until ~7–5 Ma as inferred from fine-grained deposits north of the Sudetes (Dyjor, 1970; Badura and Przybylski, 2004).

6.3. Wider regional context

The Karkonosze Mts. are just one among many basement blocks in the Variscan belt of Western and Central Europe with poor temporal constraints on the long-term history of uplift, erosion and planation. Ziegler and co-workers forwarded several theories on the long-term geological and geomorphological evolution of this part of Europe (Malkovský, 1987; Ziegler, 1990; Ziegler and Dèzes, 2007; Ziegler et al., 1998, 2002). After a prolonged period of tectonic quiescence throughout most of the Mesozoic, uplift began in the Turonian and continued until its peak in the Palaeocene (Ziegler and Dèzes, 2007). Our data are consistent with the age of the onset of a major tectonic event, but in the Karkonosze this phase was not as enduring and tectonic relief was created and destroyed much earlier (within the Cretaceous) than suggested by Ziegler and Dèzes (2007).

The next important geological event dated at Late Eocene to Early Miocene was widespread volcanism, particularly in the Eger (Ohře) Graben (Adamovič and Coubal, 1999; Ulrych et al., 1999), and Sudetes (Badura et al., 2005). Surprisingly, we do not see any effect of volcanism in our dataset from the summit surface, as the samples do not show signs of re-heating, although two of our samples (K-7 and K-12) are located fairly close to a sub-volcanic basanite body dated at 26 Ma by K–Ar method (see Fig. 3; Pécskay et al., 2004).

Similarly, we do not see clear thermochronological evidence of the most recent, Late Neogene differential uplift and subsidence, inferred from the present-day landform pattern and sedimentary record around the Sudetes.

The period of accelerated exhumation in the Late Cretaceous so well documented in the Karkonosze, has equivalents in other Variscan massifs in the Central Europe. It was identified in the Harz Mts. (AFT ages: 73–83 Ma with generally long mean track lengths; Thomson et al., 1997), Ruhla Crystalline Complex (AFT ages: 69–81 Ma with generally long mean track lengths; Thomson and Zeh, 2000), Lower Saxony Basin (AFT ages: 89–72 Ma; Senglaub et al., 2005), Fichtelgebirge in the western border of the Bohemian Massif (Coyle et al., 1997; Hejl et al., 1997), and along the Franconian Line (Bischoff, 1993; Wagner et al., 1989). Petrographic and geochemical data from stratigraphically well-calibrated sediments of 82–86 Ma age (von Eynatten et al., 2008) precisely constrain the erosion record in the Harz Mts. Collectively, they suggest that the Late Cretaceous was a period of major environmental change, with topographic relief forming and decaying fairly rapidly.

The picture is less clear towards the Eger volcano-tectonic zone, where rift-related thermal activity likely rejuvenated AFT system to various degrees (e.g., Filip et al., 2007), making the interpretation of data difficult. Lange et al. (2008) reported 96 AFT ages from a relatively small area of Saxonian basement with 4 age populations of ~65, ~95, ~135, ~180 Ma, but no geodynamic interpretation of the data is presented. Ventura and Lisker (2003) reported 8 AFT ages from a borehole in Erzgebirge and argued for two-stage cooling in the Late Jurassic–Late Cretaceous and Late Tertiary, and Aramowicz et al. (2006) reported 6 apparent AFT ages of 43–57 Ma from the Sowie Mountains, in the vicinity of the major neotectonic structure (Sudetic Marginal Fault).

7. Summary and implications for models of long-term landform evolution

The long-term geomorphic history of ancient basement massifs, despite their prominent role in the history of geomorphology, is relatively poorly constrained. Our study of the Karkonosze, which combines three thermochronometers, provides important time limitations and insights into the genetic evolution of these massifs.

First, we were able to track the geomorphic record in this intraplate setting back to the middle Cretaceous and, as indicated by middle Cretaceous ZHe ages, place a >5 km constraint on the erosion since that time.

Second, by using complementary thermochronometers we obtained clear evidence that denudation rates varied over several orders of magnitude throughout end-Mesozoic and Cenozoic. Although AFT data show that >3.6 km of rock has been eroded since the Turonian, they provide no solid basis to infer the temporal pattern of erosion over the 90 Ma. However, the (U–Th–[Sm])/He data show that much of this thickness was eroded very quickly (within 10–15 Ma) and to the present, little denudation has occurred.

Third, we can speculate about reasons for the high rates of exhumation and erosion between 90 and 75 Ma ago. The principal trigger for accelerating erosion was most likely uplift, however, efficient denudation and relief rejuvenation does not necessarily require high intensity landforming processes. The Cretaceous in Central Europe was a period characterised by tropical and humid environmental conditions, suitable for deep weathering of granite and other bedrock (Migoń and Lidmar-Bergström, 2001). Landform evolution may have been accomplished via efficient conversion of rock to saprolite, frequent shallow landslides, gullying and fluvial dissection of deeply weathered terrain. Perhaps basement terrains in low latitude, humid sections of passive margins, such as in south-eastern Brazil (Thomas, 1995), are good analogues to the Late Cretaceous predecessors of the Karkonosze Mts.

Acknowledgements

This study was financed by the German Science Foundation. We thank Z. Engel (CAS, Prague) for his support in the sample collection, B.J. McDonald (CSIRO) for the assistance with zircon helium dating, C. Scadding and A. Thomas for their assistance with ICP MS, and to D. Mühlbayer-Renner and D. Kost (Tübingen) for their careful sample preparation. An earlier version of the manuscript benefited from the critical reviews by three anonymous reviewers.

References

Adamovič, J., Coubal, M., 1999. Intrusive geometries and Cenozoic stress history of the northern part of the Bohemian Massif. GeoLines 9, 5–14.

Aleksandrowski, P., Mazur, S., 2002. Collage tectonics in the north easternmost part of the Variscan belt: the Sudetes, Bohemian Massif. In: Winchester, J.A., Pharaoh, T.C., Verniers, J. (Eds.), Palaeozoic Amalgamation of Central Europe. Geological Society Special Publication, London, pp. 237–277.

Aramowicz, A., Anczkiewicz, A.A., Mazur, S., 2006. Fission-track dating of apatite from the Góry Sowie Massif, Polish Sudetes, NE Bohemian Massif: implications for post-Variscan denudation and uplift. Neues Jahrbuch für Mineralogie — Abhandlungen 182 (3), 221–229.

Badura, J., Przybylski, B., 2004. Late Neogene and Eopleistocene evolution of fluvial system in the Foreland of Sudetes Mts. Annales Societatis Geologorum Poloniae 74, 43–61.

Badura, J., Pécskay, Z., Koszowska, E., Wolska, A., Zuchiewicz, W., Przybylski, B., 2005. New age and petrological constraints on Lower Silesian basaltoids, SW Poland. Acta Geodynamica et Geomaterialia 2 (3/139), 7–15.

Badura, J., Zuchiewicz, W., Štěpančiková, P., Przybylski, B., Kontny, B., Cacoń, S., 2007. The Sudetic Marginal Fault: a young morphotectonic feature at the NE margin of the Bohemian Massif, Central Europe. Acta Geodynamica et Geomaterialia 4 (4), 7–29.

Belton, D.X., Brown, R.W., Kohn, B.P., Fink, D., Farley, K.A., 2004. Quantitative resolution of the debate over antiquity of the central Australian landscape: implications for the tectonic and geomorphic stability of cratonic interiors. Earth and Planetary Science Letters 219, 21–34.

Berg, G., 1938. Erläuterungen zu Blatt Landeshut. Lieferung, 193. Preussisches Geolologisches Landesanst, Berlin.

Bischoff, R., 1993. Morphotektonische Entwicklung des Steinwaldgebietes (NE-Bayern) — Ergebnisse von Apatit-Spaltspuranalysen. Geologica Bavarica 98, 97–117.

Brown, R.W., Summerfield, M.A., Gleadow, A.J., 1994. Apatite fission track analysis: its potential for the estimation of denudation rates and implications for models of

long-term landscape development. In: Kirkby, M.J. (Ed.), Process Models and Theoretical Geomorphology. Wiley, Chichester, pp. 25–53.
Bruszewska, B., 2000. The geothermal conditions in Lower Silesia (SW Poland). Przegląd Geologiczny 48 (7), 639–643.
Büdel, J., 1957. Die "Doppelten Einebnungsflächen" in den feuchten Tropen. Zeitschrift für Geomorphologie, Neue Folge 1, 201–228.
Bull, W.B., McFadden, L.D., 1977. Tectonic geomorphology north and south of the Garlock fault, California. In: Doehring, D.O. (Ed.), Geomorphology in Arid Regions. Allen and Unwin, London, pp. 115–138.
Burtner, R.L., Nigrini, A., Donelick, R.A., 1994. Thermochronology of Lower Cretaceous source rocks in the Idaho–Wyoming thrust belt. AAPG Bulletin 78 (10), 1613–1636.
Chrząstek, A., 2002. Stratygrafia i warunki sedymentacji retu oraz dolnego wapienia muszlowego niecki północnosudeckiej. Acta Universitatis Wratislaviensis 2383, Prace Geologiczno-Mineralogiczne 73.
Cloos, H., 1925. Einführung in die tektonische Behandlung magmatischer Erscheinungen (Granittektonik). Verlag von Gebrüder Borntraeger, Berlin.
Coubal, M., 1990. Compression along faults: example from the Bohemian Cretaceous Basin. Mineralia Slovaca 22, 139–144.
Coyle, D.A., Wagner, G.A., Hejl, E., Brown, R., Van den haute, P., 1997. The Cretaceous and younger thermal history of the KTB site (Germany): apatite fission-track data from the Vorbohrung. Geologische Rundschau 86, 203–209.
Danišík, M., 2005. Cooling history and relief evolution of Corsica (France) as constrained by fission track and (U–Th)/He thermochronology. Tübinger Geowissenschaftliche Arbeiten, Reihe A 72, 1–130.
Danišík, M., Kuhlemann, J., Dunkl, I., Székely, B., Frisch, W., 2007. Burial and exhumation of Corsica (France) in the light of fission track data. Tectonics 26 (TC1001), 1–24. doi:10.1029/2005TC001938.
Danišík, M., Sachsenhofer, R.F., Privalov, V.A., Panova, E.A., Frisch, W., Spiegel, C., 2008. Low-temperature thermal evolution of the Azov Massif (Ukrainian Shield – Ukraine) — implications for interpreting (U–Th)/He and fission track ages from cratons. Tectonophysics 456, 171–179.
Demek, J., 1975. Planation surfaces and their significance for the morphostructural analysis of the Czech Socialist Republic (ČSR). Studia Geographica 54, 133–164 ČSAV Brno.
Désire-Marchand, J., Klein, C., 1987. Fichtelgebirge, Böhmerwald, Bayerischer Wald. Contribution à l'étude du problème des Piedmonttreppen. Zeitschrift für Geomorphologie, Neue Folge, Suppl. Bd. 65, 101–138.
Dèzes, P., Schmid, S.M., Ziegler, P.A., 2004. Evolution of the Cenozoic Rift System: interaction of the Alpine and Pyrenean orogens with their foreland lithosphere. Tectonophysics 389, 1–33.
Donelick, R.A., Ketcham, R.A., Carlson, W.D., 1999. Variability of apatite fission-track annealing kinetics: I. Experimental results. American Mineralogist 84, 1224–1234.
Dudek, A., Suk, M., 1965. The depth relief of the granitoid plutons of the Moldanubicum. Neues Jahrbuch für Geologie und Paläontologie — Abhandlungen 123 (1), 1–19.
Dunkl, I., 2002. TRACKKEY: a Windows program for calculation and graphical presentation of fission track data. Computers and Geosciences 28 (2), 3–12.
Duthou, J.-L., Couturie, J.P., Mierzejewski, M.P., Pin, C., 1991. Next dating of granite samples from the Karkonosze Mountains using Rb–Sr total rock's isochrone method [in Polish] Przegląd Geologiczny 39, 75–78.
Dyjor, S., 1970. Seria poznańska w Polsce zachodniej. Kwartalnik Geologiczny 12, 819–835.
Dyjor, S., Dyjor, S., 1975. Late Tertiary tectonic movements in the Sudety Mts. and Fore-Sudetic Block. in Polish with English summary In: Kowalski, W.C. (Ed.), Recent and Neotectonic Crustal Movements in Poland. Wydawnictwa Geologiczne, Warszawa, pp. 121–132.
Eitel, B., 2002. Flächensystem und Talbildung im östlichen Bayerischen Wald (Großraum Passau–Freyung). In: Ratusny, A. (Ed.), Flußlandschaften an Inn und Donau. : Passauer Kontaktstudium Erdkunde, 6. Passau, pp. 19–34.
Evans, N.J., Byrne, J.P., Keegan, J.T., Dotter, L.E., 2005. Determination of uranium and thorium in zircon, apatite, and fluorite: application to laser (U–Th)/He thermochronology. Journal of Analytical Chemistry 60 (12), 1159–1165.
Farley, K.A., 2000. Helium diffusion from apatite: general behavior as illustrated by Durango fluorapatite. Journal of Geophysical Research 105 (B2), 2903–2914.
Farley, K.A., 2002. (U–Th)/He dating: techniques, calibrations, and applications. Reviews in Mineralogy and Geochemistry 47, 819–844.
Farley, K.A., Wolf, R.A., Silver, L.T., 1996. The effect of long alpha-stopping distances on (U–Th)/He ages. Geochimica et Cosmochimica Acta 60 (21), 4223–4229.
Faupl, P., Wagreich, M., 1999. Late Jurassic to Eocene palaeogeography and geodynamic evolution of the Eastern Alps. Mitteilungen der Österreichischen Geologischen Gesellschaft 92, 79–94.
Filip, J., Ulrych, J., Adamovič, J., Balogh, K., 2007. Apatite fission track implications for timing of hydrothermal fluid flow in Tertiary volcanics of the Bohemian Massif. Journal of Geosciences 52, 211–220.
Foeken, J.P.T., Persano, C., Stuart, F.M., ter Voorde, M., 2007. Role of topography in isotherm perturbation: apatite (U–Th)/He and fission track results from the Malta tunnel, Tauern Window, Austria. Tectonics 26. doi:10.1029/2006TC002049.
Galbraith, R.F., Laslett, G.M., 1993. Statistical models for mixed fission track ages. Nuclear Tracks and Radiation Measurements 21, 459–470.
Glasmacher, U., Mann, U., Wagner, G.A., 2002. Thermotectonic evolution of the Barrandian, Czech Republic as revealed by apatite fission-track analysis. Tectonophysics 359, 381–402.
Gleadow, A.J.W., 1981. Fission-track dating methods: what are the real alternatives? Nuclear Tracks and Radiation Measurements 5 (1/2), 3–14.
Gunnell, Y., Calvet, M., Brichau, S., Carter, A., Aguilar, J.-P., Zeyen, H., 2009. Low long-term erosion rates in high-energy mountain belts: Insights from thermo- and biochronology in the Eastern Pyrenees. Earth and Planetary Science Letters 278, 208–218.
Hejl, E., Coyle, D., Lal, N., Van den haute, P., Wagner, G.A., 1997. Fission-track dating of the western border of the Bohemian massif: thermochronology and tectonic implications. Geologosche Rundschau 86, 210–219.
Hourigan, J.K., Reiners, P.W., Brandon, M.T., 2005. U–Th zonation-dependent alpha-ejection in (U–Th)/He chronometry. Geochimica et Cosmochimica Acta 69, 3349–3365.
Hurford, A.J., Green, P.F., 1983. The zeta age calibration of fission-track dating. Chemical Geology 41, 285–312.
Jarmołowicz-Szulc, K., 1984. Geochronological study of a part of the northern cover of the Karkonosze granite by fission track method [in Polish]. Archiwum Mineralogiczne 39, 139–183.
Jessen, O., 1938. Tertiärklima und Mittelgebirgsmorphologie. Zeitschrift der Gesellschaft für Erdkunde 1938, 36–48.
Ketcham, R.A., 2005. Forward and inverse modeling of low-temperature thermochronometry data. In: Reiners, P.W., Ehlers, T.A. (Eds.), Low-Temperature Thermochronology: Techniques, Interpretations, and Applications. Reviews in Mineralogy and Geochemistry 58, 275–314.
Ketcham, R.A., Donelick, R.A., Carlson, W.D., 1999. Variability of apatite fission track annealing kinetics: III. Extrapolation to geologic time scales. American Mineralogist 84, 1235–1255.
Klimaszewski, M., 1958. Rozwój terytorium Polski w okresie przedczwartorzędowym. Przegląd Geograficzny 30, 3–43.
Kozdrój, W., Krentz, O., Opletal, M., 2001. Geological map and Comments on the Geological map Lausitz, Jizera, Karkonosze (without Cenozoic sediments) 1:100000. Państwowy Instytut Geologiczny, Warsaw.
Krzywiec, P., 2006. Structural inversion of the Pomeranian and Kuiavian segments of the Mid-Polish Trough - lateral variations in timing and structural style. Geological Quarterly 50, 151–167.
Kuhlemann, J., 2000. Post-collisional sediment budget of circum-Alpine basins (Central Europe). Memorie di Scienze Geologiche (Padova) 52, 1–91.
Lange, J.-M., Tonk, Ch., Wagner, G.A., 2008. Apatite fission track data for the Postvariscan thermotectonic evolution of the Saxon basement — first results [in German]. Zeitschrift der Deutschen Gesellschaft für Geowissenschaften 159 (1), 123–132.
Maheľ, M., 1973. Tectonic map of the Carpathian–Balkan mountain system and adjacent areas, 1:1000000. Bratislava, GUDS Bratislava and UNESCO, Vienna.
Malkovský, M., 1987. The Mesozoic and Tertiary basins of the Bohemian Massif and their evolution. Tectonophysics 137, 31–42.
Mazur, S., Scheck-Wenderoth, M., Krzywiec, P., 2005. Different modes of the Late Cretaceous–Early Tertiary inversion in the North German and Polish basins. International Journal of Earth Sciences 94, 782–798.
Mazur, S., Aleksandrowski, P., Kryza, R., Oberc-Dziedzic, T., 2006. The Variscan orogen in Poland. Geological Quarterly 50, 89–118.
Mazur, S., Aleksandrowski, P., Turniak, K., Awdankiewicz, M., 2007. Geology, tectonic evolution and Late Palaeozoic magmatism of the Sudetes — an overview. In: Kozłowski, A., Wiszniewska, J. (Eds.), Granitoids in Poland. Archivum Mineralogiae Monograph No. 1, Committee of Mineralogical Sciences of the Polish Academy of Sciences — Faculty of Geology of the Warsaw University. Polish Geological Institute, Warszawa, pp. 59–87.
Mierzejewski, M.P., 1985. Denudation of the ancient Karkonosze Mts during Permo-Carboniferous and Mesozoic era [in Polish]. Geologia Sudetica 20 (1), 197–225.
Migoń, P., 1999. The role of 'preglacial' relief in the development of mountain glaciation in the Sudetes, with the special reference to the Karkonosze mountains. Zeitschrift für Geomorphologie, Neue Folge, Supplementbände, Band 113, 33–44.
Migoń, P., Hrádek, M., Parzóch, K., 2002. Extreme geomorphic events in the Sudetes Mountains and their long-term impact. Studia Geomorphologica Carpatho-Balcanica 36, 29–49.
Migoń, P., Lidmar-Bergström, K., 2001. Weathering mantles and their significance for geomorphological evolution of central and northern Europe since the Mesozoic. Earth Science Reviews 56, 285–324.
Milewicz, J., 1997. Górna kreda depresji północnosudeckiej (lito- i biostratygrafia, paleogeografia, tektonika oraz uwagi o surowcach). Prace Geologiczno-Mineralogiczne 61, 1–58.
Partsch, J., 1894. Die Vergletscherung des Riesengebirges zur Eiszeit. Forsch. z. Deutsch. Landes u. Volkskunde 8 (2), 103–194.
Pécskay, Z., Lorenc, M.W., Birkenmajer, K., Zagożdżon, P.P., 2004. Recent geochronological studies of Tertiary volcanics in Lower Silesia, Poland. International Workshop "Basalts 2004", Conference Materials, Leśna, pp. 24–25.
Penck, W., 1925. Die Morphologische Analyse. Engelhorn, Stuttgart.
Placek, A., Migoń, P., 2007. Rock-landform relationships in the Sudetes in the light of rock strength assessment using the Schmidt hammer. In: Goudie, A.S., Kalvoda, J. (Eds.), Geomorphological Variations. Nakladatelství P3K, Prague, pp. 287–311.
Prosová, M., 1974. Geneze reliktního terciéru. Univerzita Karlova, Prague.
Reiners, P.W., 2005. Zircon (U–Th)/He thermochronometry. In: Reiners, P.W., Ehlers, T.A. (Eds.), Low-temperature thermochronology: techniques, interpretations, and applications: Reviews in Mineralogy and Geochemistry, 58, pp. 151–176.
Reiners, P.W., Spell, T.L., Nicolescu, S., Zanetti, K.A., 2004. Zircon (U–Th)/He thermochronometry: He diffusion and comparisons with $^{40}Ar/^{39}Ar$ dating. Geochimica et Cosmochimica Acta 68, 1857–1887.
Resak, M., Narkiewicz, M., Littke, R., 2008. New basin modelling results from the Polish part of the Central European Basin system: implications for the Cretaceous–Early Paleogene structural inversion. International Journal of Earth Sciences 97, 955–972.
Sekyra, J., 1964. Kvarternì geologické a geomorfologické problemy krkonošského krystalinika. Opera Corcontica 1, 7–24.
Senglaub, Y., Brix, M.R., Adriasola, A.C., Littke, R., 2005. New information on the thermal history of the southwestern Lower Saxony Basin, northern Germany, based on fission track analysis. International Journal of Earth Sciences 94, 876–896.

Skoček, V., Valečka, J., 1983. Palaeogeography of the Late Cretaceous Quadersandstein of Central Europe. Palaeogeography, Palaeoclimatology, Palaeoecology 44, 71–92.
Summerfield, M.A., 2000. Geomorphology and global tectonics: introduction. In: Summerfield, M.A. (Ed.), Geomophology and Global Tectonics. Wiley, Chichester, pp. 3–12.
Śliwiński, W., 1980. A model for caliche formation in the continental Permian deposits of southeastern Intra-Sudetic Basin, southwestern Poland. Geologia Sudetica 15 (2), 83–104.
Thomas, M.F., 1995. Models for landform development on passive margins. Some implications for relief development in glaciated areas. Geomorphology 12 (1), 3–15.
Thomson, S.N., Brix, M.R., Carter, A., 1997. Late Cretaceous denudation of the Harz Massif assessed by apatite fission-track analysis. Schriftenreihe der DGG 2, 115.
Thomson, S.N., Zeh, A., 2000. Fission-track thermochronology of the Ruhla crystalline complex: new constraints on the post-Variscan thermal evolution of the NW Saxo–Bohemian Massif. Tectonophysics 324, 17–35.
Uličný, D., 2001. Depositional systems and sequence stratigraphy of coarse-grained deltas in a shallow-marine, strike-slip setting: the Bohemian Cretaceous Basin, Czech Republic. Sedimentology 48, 599–628.
Uličný, D., Čech, S., Grygar, R., 2003. Tectonics and depositional systems of a shallow-marine, intra-continental strike-slip basin: exposures of the Český Ráj Region, Bohemian Cretaceous Basin. Geolines 16, 133–148.
Ulrych, J., Pivec, E., Lang, M., Balogh, K., Kropacek, V., 1999. Cenozoic intraplate volcanic rocks series of the Bohemian Massif: a review. GeoLines 9, 123–129.
Ventura, B., Lisker, F., 2003. Long-term landscape evolution of the northeastern margin of the Bohemian Massif: apatite fission-track data from the Erzgebirge (Germany). International Journal of Earth Sciences 92, 691–700.
von Blanckenburg, F., Hewawasam, T., Kubik, P, 2004. Cosmogenic nuclide evidence for low weathering and denudation in the wet, tropical highlands of Sri Lanka. Journal of Geophysical Research 109 (F03008), 1–22.
von Eynatten, H., Voigt, T., Meier, A., Franzke, H.-J., Gauppet, R., 2008. Provenance of Cretaceous clastics in the Subhercynian Basin: constraints to exhumation of the Harz Mountains and timing of inversion tectonics in Central Europe. International Journal of Earth Sciences 97, 1315–1330.
Wagner, G.A., Michalsky, I., Zaun, P., 1989. Apatite fission-track dating of the central European basement. Postvariscan thermotectonic evolution. In: Emmermann, R., Wohlenberg, J. (Eds.), The German Continental Deep Drilling project (KTB). Springer, Berlin Heidelberg New York, pp. 481–500.
Wagner, G.A., Van den haute, P., 1992. Fission-Track Dating. Enke Verlag, Stuttgart.
Wojewoda, J., 1997. Upper Cretaceous littoral-to-shelf succession in the Intrasudetic Basin and Nysa Trough, Sudety Mts. In: Wojewoda, J. (Ed.), Obszary źródłowe: zapis w osadach. Wind, Wrocław, pp. 81–96.
Wolf, R.A., Farley, K.A., Kass, D.M., 1998. Modeling of the temperature sensitivity of the apatite (U–Th)/He thermochronometer. Chemical Geology 148, 105–114.
Ziegler, P.A., 1990. Geological Atlas of Western and Central Europe. Shell Internationale Petroleum Maatschappij B.V., Geological Society, London.
Ziegler, P.A., Dèzes, P., 2007. Cenozoic uplift of Variscan Massifs in the Alpine foreland: timing and controlling mechanisms. Global and Planetary Change 58, 237–269.
Ziegler, P.A., van Wees, J.-D., Cloetingh, S., 1998. Mechanical controls on collision related compressional intraplate deformation. Tectonophysics 300, 103–129.
Ziegler, P.A., Bertotti, G., Cloetingh, S., 2002. Dynamic processes controlling foreland development: the role of mechanical (de)coupling of orogenic wedges and forelands. In: Bertotti, G., Schulmann, K., Cloetingh, S. (Eds.), Continental Collision and the Tectono-Sedimentary Evolution of Forelands. European Geophysical Society. Stephan Mueller Special Publication 1, 29–91.
Zuchiewicz, W., Badura, J., Jarosiński, M., 2007. Neotectonics of Poland: an overview of active faulting. Studia Quaternaria 24, 5–20.
Žák, J., Vyhnálek, B., Kabele, P., 2006. Is there a relationship between magmatic fabrics and brittle fractures in plutons? A view based on structural analysis, anisotropy of magnetic susceptibility and thermo-mechanical modelling of the Tanvald pluton (Bohemian Massif). Physics of the Earth and Planetary Interiors 157, 286–310.